$CD105^+$ cells, demonstrating over 98% at the sixth passage. When single $CD105^+$ cells were plated in 35 mm dishes coated with type I collagen they formed colonies in ten days. This demonstrates the colony formation ability of these CD 105^+ cells. The efficiency of attachment and growth of pulp 105^+, adipose $CD105^+$ and pulp $CD105^-$ cells was estimated to be 8%, 3.7%, 1%, respectively. Limiting dilution analysis at the third passage culture showed that the frequency of CFU in pulp $CD105^+$ cells was estimated to be 80%, while that in total pulp cells 30%, and that in adipose $CD105^+$ cells 50%.

To characterize the "stemness" of pulp $CD105^+$ cells, cell surface antigen markers were examined by flow cytometry and compared with adipose $CD105^+$ cells and total pulp cells. Pulp $CD105^+$ cells, adipose $CD105^+$ cells and total pulp cells were positive for CD29, CD44, CD90 and CD105, and negative for CD31 at the third passage, which are minimal criteria for mesenchymal stem cells. It is noteworthy that the percentage of pulp $CD105^+$ cells which expressed CD73, CD150 and CXCR4 were much higher compared with adipose $CD105^+$ cells and total pulp cells (Table 1). The expression of stem cell markers, *CXCR4, Sox2, and Bmi1* mRNA was 16.8, 64 and 3.5 times higher in pulp $CD105^+$ cells than those in total pulp cells, respectively, suggesting the stem cell properties of pulp $CD105^+$ cells. Further, the pulp-derived $CD105^+$ cells exhibited higher expression of the characteristic stem cell markers compared to the adipose-derived $CD105^+$ cells. Angiogenic factors and/or neurotrophic factors, *VEGF-A, GM-CSF, nerve growth factor (NGF), brain-derived neurotrophic factor (BDNF), neuropeptide Y, neurotrophin 3, E-selectin*, and *VCAM-1* were expressed higher in pulp $CD105^+$ cells compared with total pulp cells and adipose $CD105^+$ cells (Fig. 2).

The differentiation of pulp $CD105^+$ cells into adipose cells (Fig. 3A, D), endothelial cells (Fig. 3E), neuronal cells (Fig. 3H, J, K) and odontoblast/osteoblast lineage (Fig. 3L, O) was observed. However, the mineralized matrix was higher in total pulp cells (Fig. 3M) than that in pulp $CD105^+$ cells (Fig. 3L). Adipose $CD105^+$ cells demonstrated adipogenic (Fig. 3C, D)

and osteogenic potential (Fig. 3N, O) but neither angiogenic (Fig. 3G) nor neurogenic potential. The proliferation activity with SDF-1 was higher in pulp $CD105^+$ cells than that in total pulp cells and adipose $CD105^+$ cells (Fig. 3P). The migration activity with SDF-1 shown in the TAXIScan-FL was much higher in pulp $CD105^+$ cells compared with total pulp cells and adipose $CD105^+$ cells (Supplemental Video A-C).

Pulp Regeneration after Transplantation of Pulp $CD105^+$ Cells in the Root Canal

We next demonstrated by the in vivo transplantation of autologous pulp $CD105^+$ cells with SDF-1 into the root canal of mature teeth induced complete apical closure after pulpectomy in dogs (Fig. 4). Pulp $CD105^+$ cells formed pulp-like tissue by day 14 when transplanted with SDF-1 (Fig. 5A-C). However, transplantation of $CD105^+$ cells alone (Fig. 5E), or SDF-1 alone (Fig. 5F) yielded less pulp. Statistical analysis showed that the regenerated area was significantly larger (3.3-fold and 4.2-fold increase) when pulp $CD105^+$ cells were transplanted with SDF-1 compared with $CD105^+$ cells alone or SDF-1 alone, respectively (Fig. 6). The odontoblast-like cells attached to the dentinal wall in the root canal, extending their processes into dentin tubules (Fig. 5D). The pulp-like tissue was further extended to the cementum-enamel junction under the cement filling 90 days after transplantation of pulp $CD105^+$ cells together with SDF-1 (Fig. 5G). The cells in the upper part of the regenerated tissue were spindle shaped (Fig. 5H), and those in the middle part were stellate-like (Fig. 5I) similar to those in the normal pulp (Fig. 5J). It is noteworthy that tubular dentin was observed along the dentinal wall (Fig. 5G, K). The odontoblasts lining the dentinal wall were positive for *enamelysin/matrix metalloproteinase (MMP) 20* (Fig. 5L) and *Dspp* (Fig. 5M), two markers for odontoblasts. However, if unfractionated total pulp cells are transplanted instead of $CD105^+$ cells less tissue was observed (Fig. 5N, O), followed by evidence of mineralization on day 90 (Fig. 5Q, R). Similarly when adipose tissue-derived $CD105^+$ cells

were transplanted, much less regenerate tissue was observed (Fig. 5P). Further statistical analysis showed that the ratio of newly regenerated tissue to root canal surface area was significantly larger (51.6-fold and 2.2-fold increase) in the case of pulp $CD105^+$ cell transplantation with SDF-1 than in the case of transplantation of adipose $CD105^+$ cells with SDF-1 or total pulp cells with SDF-1 on day 14 (Fig. 6). Confocal laser microscopic analysis after staining with BS-1 lectin of cryosections demonstrated neovascularization in the regenerated tissue (Fig. 7A). Two-photon microscopic analysis showed that numerous DiI-labeled transplanted pulp $CD105^+$ cells were in the vicinity of the newly formed capillaries (Fig. 7B), implicating a trophic role for these cells in neovascularization. The three dimensional image of induced vascularization in the regenerated tissue on day 14 (Fig. 7D) was similar in density and orientation to that in the normal pulp (Fig. 7E). The transplanted $CD105^+$ cells were observed overall in the newly regenerated pulp (Fig. 7C), suggesting their potential capacity to migrate to the upper site by SDF-1. The neuronal process stained by PGP9.5 antibody was extended into the newly regenerated pulp from apical foramen (Fig. 7F). DiI labeling on the regenerated pulp in the lower third incisor in vivo showed the neuronal process from regenerated pulp connecting to inferior alveolar nerve (Fig. 7G).

Two Dimensional Electrophoretic Protein Analyses and Gene Expression Analyses of Pulp Regeneration

Two dimensional electrophoretic analyses demonstrated that the qualitative and quantitative protein pattern of regenerated pulp tissue on day 28 was similar to that of normal pulp tissue derived from the same individual. The protein spots detected both in normal and regenerated pulp tissue represented 85.5% (123 spots) (Supplemental Fig. 1A-C). On the other hand, there were some differences in the protein spots of normal pulp tissue compared to periodontal ligament (Supplemental Fig. 1D-F).

There have been no specific markers for pulp. Thus, some specific markers for periodontal ligament were used to further confirm normal pulp regeneration. Expression of *axin2*[13], *periostin*[14], and *asporin/periodontal ligament-associated protein 1 (PLAP-1)*[15] mRNA were much higher (25,531-fold, 179-fold and 11-fold) in normal periodontal ligament than those in the regenerated tissue on day 28, respectively. Those genes were similarly expressed in a very low level in normal pulp compared to the regenerated tissue (0.4-fold, 0.4-fold, and 2.4-fold, respectively) (Fig. 8A). *Collagen αI(I)* was 9.3 times more expressed in periodontal ligament compared with the regenerated tissue, although this expression was not different between normal pulp and the regenerated tissue (Fig. 8A). *Syndecan3* and *TenascinC*, known to be highly expressed in pulp[16, 17], were 14.3 times and 50.0 times more expressed in the regenerated tissue compared with periodontal ligament, although those expressions in the regenerated tissue were similar to those in normal pulp (Fig. 8B). Hierachical clustering based on Affymetrix data produced a clear pattern separation of normal pulp tissue and the regenerated tissue from periodontal ligament (Supplemental Fig. 1G). Thus, the two dimensional electrophoretic analyses and the gene expression analyses suggested that the regenerated pulp tissue was identical to true functional normal pulp.

DISCUSSION

Regeneration of pulp tissue is an unmet need in endodontic therapy. The critical requirements for pulp regeneration are morphogenesis of pulp tissue replete with angiogenesis/vasculogenesis and neurogenesis[3, 18]. The induction of pulp-like tissue has been reported in a tooth slice model of subcutaneous transplantation in immunodeficient mice, by filling of pulp stem cells and dentin matrix protein 1 (DMP1) together[19] or stem cells from exfoliated deciduous teeth only[20] in a thin tooth slice. Similarly another model for the induction of pulp-like tissue was subcutaneously transplantation of human tooth root

fragment (6-7 mm long) with an enlarged root canal (1.0-1.25 mm in diameter) with one end sealed with mineral trioxide aggregate (MTA) cement. Stem/progenitor cells from apical papilla and dental stem cells were inserted into the root. Pulp-like tissue with well-established vascularity and a continuous layer of odontoblast-like cells along the dentinal wall were observed demonstrating the feasibility of pulp regeneration[21]. The novel findings in this investigation was the complete regeneration of whole pulp tissue following pulpectomy without tooth extraction by autologous pulp $CD105^+$ cell transplantation with SDF-1 in mature teeth with complete apical closure.

Human pulp $CD105^+$ cells have demonstrated angiogenesis/vasculogenic and neurogenic potential[8]. The SDF-1-CXCR4 axis plays a role in stem cell homing even in adulthood especially after ischemia[22]. In this investigation, *CXCR4* was highly expressed in canine pulp $CD105^+$ cells. The regenerated pulp-like tissue was more in pulp $CD105^+$ cells with SDF-1 compared with $CD105^+$ cells alone or SDF-1 alone. Therefore, these results suggested combinatory effect of SDF-1 and pulp $CD105^+$ cells, especially SDF-1-CXCR4 axis for whole pulp regeneration. Similar contributions of SDF-1-CXCR4 axis, the 'homing' of stem cells expressing CXCR4 to a hypoxic-ischemic lesion where expression of SDF-1 significantly increased, have been reported in the rat ischemic brain following transplantation of human umbilical cord blood cells[23], and in the myocardial ischemia[24] or a subfraction of side population cells[25].

Pulp tissue is readily available from discarded permanent teeth such as third molar and deciduous teeth after extraction. The autologous pulp stem cell source, however, is limited to patients who have discarded teeth with adequate pulp. ~~The cell surface antigen markers for stem cells, CD44, CD90 were highly expressed both in pulp and adipose $CD105^+$ cells, while CD73 and CD150, were much highly expressed in pulp $CD105^+$ cells compared with adipose $CD105^+$ cells.~~ Higher ratio of CD73 and CD150 positive cells and higher expression of ~~stem~~

~~cell markers,~~ *CXCR4*, *Sox2*, and *Bmi1* mRNA ~~and were expressed higher~~ in pulp CD105$^+$ cells compared to adipose CD105$^+$ cells, suggesting more stemness of pulp CD105$^+$ cells. Higher angiogenic and neurogenic potential ~~in vitro were higher in pulp CD105$^+$ cells than those in adipose CD105$^+$ cells and total pulp cells.~~ and higher expression of a variety of proangiogenic factors and neurotrophic factors ~~much higher~~ in pulp CD105$^+$ cells compared to adipose CD105$^+$ cells in vitro, and expression of cytokines, *VEGF-A* and *GM-CSF* mRNA ~~were expressed~~ by the transplanted pulp stem cells in the vicinity of the newly formed vasculature in the regenerated pulp[26], implying the higher

trophic actions of pulp CD105$^+$ cells on endothelial cells to promote neovascularization. Thus, pulp CD105$^+$ cells are more useful cell source in induction of pulp regeneration by cell therapy compared with adipose CD105$^+$ cells and total pulp cells.

The routine translation of the current findings to the clinic is dependent on the use of autologous pulp in normal healthy patients. However, in the aged and in diabetic patients the pulp tissue may be limiting and may require novel approaches.

CONCLUSION

Our data demonstrates for the first time that pulp CD105$^+$ cells with SDF-1 induce complete pulp regeneration replete with neurogenesis and vasculogenesis in vivo in the adult dog following experimental pulpectomy. This cell therapy demonstrates the potential clinical utility of fractionated CD105$^+$ cells for endodontic treatment for conservation of teeth in dentistry.

ACKNOWLEDGMENTS

This work was supported by grants of Collaborative Development of Innovative Seeds, Potentiality verification stage from Japan Science and Technology Agency, a Grant-in-Aid for

Scientific Research from the Ministry of Education, and the Research Grant for Longevity Sciences (21A-7) from the Ministry of Health, Labour and Welfare (M.N.), Science, Sports and Culture, Japan, #20390504 (M.N.), #21791872 (K.I.).

DISCLOSURE OF POTENTIAL CONFLICTS OF INTEREST

The authors indicate no potential conflicts of interest.

REFERENCES

1. Nakashima, M., Akamine, A. The application of tissue engineering to regeneration of pulp and dentin in endodontics. J Endod **31,** 711, 2005.
2. Nakashima, M., Reddi, AH. The application of bone morphogenetic proteins to dental tissue engineering. Nature Biotech **21,** 1025, 2003.
3. Hargreaves, KM., Giesler, T., Henry, M., Wang, Y. Regeneration potential of the young permanent tooth: what does the future hold? J Endod **34,** S51, 2008.
4. Huang, GT. Apexification: the beginning of its end. Int Endod J **42,** 855, 2009.
5. Barry, FP., Boynton, RE., Haynesworth, S., Murphy JM., Zaia J. The monoclonal antibody SH-2, raised against human mesenchymal stem cells, recognizes an epitope on endoglin (CD105). Biochem Biophys Res Commun **265**, 134, 1999.
6. Wynn, RF., Hart, CA., Corradi-Perini, C., O'Neil,l L., Evans, CA., Wraith, JE., Fairbairn, LJ., Bellantuono, I. A small proportion of mesenchymal stem cells strongly expresses functionally active CXCR4 receptor capable of promoting migration to bone marrow. Blood **104,** 2643, 2004.
7. Dar, A., Goichberg, P., Shinder, V., Kalinkovich, A., Kollet, O., Netzer, N., Margalit, R., Zsak, M., Nagler, A., Hardan, I., Resnick, I., Rot, A., Lapidot, T. Chemokine receptor

CXCR4-dependent internalization and resecretion of functional chemokine SDF-1 by bone marrow endothelial and stromal cells. Nat Immunol **6,** 1038, 2005.

8. Nakashima, M., Iohara, K., Sugiyama, M. Human dental pulp stem cells with highly angiogenic and neurogenic potential for possible use in pulp regeneration. Cytokine & Growth Factor Reviews **20,** 435, 2009.
9. Lima, e, Silva, R., Shen, J., Hackett, SF., Kachi, S., Akiyama, H., Kiuchi, K., Yokoi, K., Hatara, MC., Lauer, T., Aslam, S., Gong, YY., Xiao, WH., Khu, NH., Thut, C., Campochiaro, PA. The SDF-1/CXCR4 ligand/receptor pair is an important contributor to several types of ocular neovascularization. FASEB J **21,** 3219, 2007.
10. van, Weel, V., Seghers, L., de, Vries, MR., Kuiper, EJ., Schlingemann, RO., Bajema, IM., Lindeman, JH., Delis-van, Diemen, PM., van, Hinsbergh, VW., van, Bocke,l JH., Quax, PH. Expression of vascular endothelial growth factor, stromal cell-derived factor-1, and CXCR4 in human limb muscle with acute and chronic ischemia. Arterioscler Thromb Vasc Biol **27,** 1426, 2007.
11. Iohara, K., Zheng, L., Ito, M., Tomokiyo, A., Matsushita, K., Nakashima, M. Side population cells isolated from porcine dental pulp tissue with self-renewal and multipotency for dentinogenesis, chondrogenesis, adipogenesis, and neurogenesis. Stem Cells **24,** 2493, 2006.
12. Iohara, K., Zheng, L., Wake, H., Ito, M., Nabekura, J., Wakita, H., Nakamura, H., Into, T., Matsushita, K,, Nakashima, M. A novel stem cell source for vasculogenesis in ischemia: subfraction of side population cells from dental pulp. Stem Cells **26,** 2408, 2008.
13. Lohi, M., Tucker, AS., Sharpe, PT. Expression of Axin2 indicates a role for canonical Wnt signaling in development of the crown and root during pre- and postnatal tooth development. Dev Dyn **239,** 160, 2010.

14. Suzuki, H., Amizuka, N., Kii, I., Kawano, Y., Nozawa-Inoue, K., Suzuki, A., Yoshie, H., Kudo, A., Maeda, T. Immunohistochemical localization of periostin in tooth and its surrounding tissues in mouse mandibles during development. Anat Rec Part A **281,** 1264, 2004.

15. Nakamura, S., Terashima, T., Yoshida, T., Iseki, S., Takano, Y., Ishikawa, I., Shinomura, T. Identification of genes preferentially expressed in periodontal ligament: specific expression of a novel secreted protein, FDC-SP. Biochem Biophys Res Commun **338,** 1197, 2005.

16. Hikake, T., Mori, T., Iseki, K., Hagino, S., Zhang, Y., Takagi, H., Yokoya, S., Wanaka, A. Comparison of expression patterns between CREB family transcription factor OASIS and proteoglycan core protein genes during murine tooth development. Anat Embyol (Berl) **206,** 373, 2003.

17. Zhang, X., Schuppan, D., Becker, J., Reichart, P., Gelderblom, HR. Distribution of undulin, tenascin, and fibronectin in the human periodontal ligament and cementum: comparative immunoelectron microscopy with ultra-thin cryosections. J Histochem Cytochem **41,** 245, 1993.

18. Murray, PE, Garcia-Godoy, F., Hargreaves, KM. Regenerative endodontics: a review of current status and a call for action. J Endod **33,** 377, 2007.

19. Prescott RS, Alsanea R, Fayad MI, Johnson BR, Wenckus CS, Hao J, John AS, George A. In vivo generation of dental pulp-like tissue by using dental pulp stem cells, a collagen scaffold, and dentin matrix protein 1 after subcutaneous transplantation in mice. J Endod **34,** 421, 2008

20. Cordeiro, MM., Dong, Z., Kaneko, T., Zhang, Z., Miyazawa, M., Shi, S., Smith, AJ., Nör, JE. Dental pulp tissue engineering with stem cells from exfoliated deciduous teeth. J Endod **34,** 962, 2008.

21. Huang, GT., Yamaza, T., Shea, LD., Djouad, F., Kuhn, NZ., Tuan, RS., Shi, S. Stem/Progenitor cell-mediated de novo regeneration of dental pulp with newly deposited continuous layer of dentin in an in vivo model. Tissue Eng Part A **16,** 605, 2010.

22. Zaruba, MM., Franz, WM.. Role of the SDF-1-CXCR4 axis in stem cell-based therapies for ischemic cardiomyopathy. Expert Opin Biol Ther **10,** 321, 2010.

23. Rosenkranz, K., Kumbruch, S., Lebermann, K., Marschner, K., Jensen, A., Dermietzel, R., Meier, C. The chemokine SDF-1/CXCL12 contributes to the 'homing' of umbilical cord blood cells to a hypoxic-ischemic lesion in the rat brain. J Neurosci Res **88,** 1223, 2010.

24. Wang, Y., Haider, HKh., Ahmad, N., Zhang, D., Ashraf, M. Evidence for ischemia induced host-derived bone marrow cell mobilization into cardiac allografts. J Mol Cell Cardiol **41,** 478, 2006.

25. Liang, SX., Tan, TY., Gaudry, L., Chong, B. Differentiation and migration of Sca1+/CD31- cardiac side population cells in a murine myocardial ischemic model. Int J Cardiol **138,** 40, 2010.

26. Iohara, K., Zheng, L., Ito, M., Ishizaka, R., Nakamura, H., Into, T., Matsushita, K., Nakashima, M. Regeneration of dental pulp after pulpotomy by transplantation of CD31(-)/CD146(-) side population cells from a canine tooth. Regen Med **4,** 377, 2009.

Figure legend

Figure 1. Isolation of $CD105^+$ cells from adult canine dental pulp and adipose tissue. (A) The two panels show flow cytometry profiles of forward scatter (FSC) and side scatter (SSC) (left), and CD105 and SSC expression (right) on the dental pulp tissue. $CD105^+$ cells represented 6% of the total. (B) Primary pulp $CD105^+$ cell culture on day 3. (C) Primary pulp $CD105^+$ cell culture on day 10. (D) Primary total pulp cells on day 10. (E) The two panels show flow cytometry profiles of FSC and SSC (left), and CD105 and SSC expression (right)

on the adipose tissue. $CD105^+$ cells represented 5.8% of the total. (F) Primary adipose $CD105^+$ cell culture on day 3. (G) Primary adipose $CD105^+$ cell culture on day 10. (H) Primary total adipose cells on day 10. The experiments were repeated nine times and one represented experiment is presented.

Figure 2. Relative mRNA expression of cytokines of vasculogenesis and neurogenesis by real-time reverse transcription-polymerase chain reaction in pulp and adipose derived $CD105^+$ cells. The experiments were repeated four times and one represented experiment is presented.

Figure 3. Multi-lineage differentiation potential ~~of pulp cells~~. ~~The experiment was repeated three times, and one representative experiment is presented.~~ (A-D) Adipogenic potential, (E-G) Angiogenic potential, (H, I) Neurosphere formation. (J) Immunostaining with neurofilament. (D) *Adipocyte fatty acid binding protein 2* (*aP2*) mRNA expression. (K) *Neurofilament, neuromodulin* and *sodium channel, voltage-gated, type Ia* (*Scn1A*) mRNA expression. (L-N) Odontogenic/osteogenic potential. (A-C) Oil red O staining. (L-N) Alizarin red staining. (A, E, H, J, ~~K,~~ L) Pulp ~~derived~~ $CD105^+$ cells. (B, F, I, M) ~~unfractionated~~ total pulp cells. (C, G, N) Adipose ~~derived~~ $CD105^+$ cells. (P) The proliferation activity of pulp ~~derived~~ $CD105^+$ cells, ~~unfractionated~~ total pulp cells, and adipose ~~derived~~ $CD105^+$ cells with SDF-1 ~~at the final concentration of 50ng/ml~~. ~~Cell numbers were determined at 2, 12, 24, and 36 hours of culture.~~ Data are expressed as means ± SD of 4 determinations (*$P<0.01$). The experiments were repeated three times, and one representative experiment is presented.

Figure 4. Schematic diagrams of a canine model for complete pulp regeneration in permanent mature teeth. (A) pulpitis model, (B) whole pulp removal and enlargement of

apical foramen, 0.7 mm in width, (C) irrigation and filling with stem/progenitor cells in the lower part and SDF-1 in the upper part of the root canal together with collagen scaffold, (D) complete pulp regeneration.

Figure 5. Complete regeneration of pulp tissue after autologous transplantation of $CD105^+$ cells with SDF-1 in the emptied root canal after pulpectomy in dogs. (A-F) Fourteen days after transplantation. (A-D) Pulp $CD105^+$ cells with SDF-1. (E) Pulp $CD105^+$ cells only. (F) SDF-1 only. (G-I, K-M) Ninety days after transplantation of pulp $CD105^+$ cells with SDF-1. (H, I) Newly formed blood vessels (v) in the upper part and the middle part of regenerated tissue. (J) Normal pulp tissue. (K) Odontoblastic cells (arrows) lining to newly formed osteodentin/tubular dentin (OD) along with the dentinal wall. (L, M) In situ hybridization analyses of odontoblast differentiation (arrows). (L) Enamelysin/MMP20. (M) Dentin sialophosphoprotein (Dspp). (N-P) Forteen days after transplantation. (N, O) Total pulp cells with SDF-1. (P) Adipose-derived $CD105^+$ cells with SDF-1. (Q, R) Ninety days after transplantation of total pulp cells with SDF-1. Mineralized tissue (arrow) and osteodentin (OD).

Figure 6. Ratio of regenerated area to root canal area on day 14. Data are expressed as means ± SD of 5 determinations. Statistical analysis was performed by the non-paired Student's t test.

Figure 7. (A) Immunostaining with BS-1 lectin. v: newly formed capillaries. (B-E) Three dimensional images of new vascularization by whole mount immunostaining with lectin. (B) Note transplanted $CD105^+$ cells in the vicinity of the newly formed capillaries. (D) The DiI labeled transplanted cells located overall in the tissue. (E) Normal pulp tissue. (F)

Immunostaining with PGP 9.5. (G) Neurogenesis in newly formed pulp tissue (white dotted line) connecting to inferior alveolar nerve.

Figure 8. Relative mRNA expression of cytokines by real-time reverse transcription-polymerase chain reaction in regenerated pulp, normal pulp and adipose periodontal tissue. The experiments were repeated four times and one represented experiment is presented.

Supplemental Figure 1. Two dimensional electrophoretic protein analyses and gene expression analyses of pulp regeneration. Two dimensional electrophoretic analysis (A-F). Representative images of proteins from normal pulp tissue (A, D), regenerated pulp-like tissue (B), and periodontal ligament (E). Overlay images of A and B (C), and D and E (F). The experiments were repeated three times and one represented experiment is presented. Hierachical cluster analysis of gene expression patterns among normal pulp, regenerated pulp-like tissue and periodontal ligament (G). A total of 42,973 probe sets are displayed. Red color indicates high level expression, green color indicates low expression, and black indicates median expression.

Supplementary video. The migration activity of pulp derived $CD105^+$ cells (A), unfractionated total pulp cells (B), and adipose derived $CD105^+$ cells (C) with SDF-1 at 10ng/μl in TAXIScan-FL®. The experiments were repeated three times and one represented experiment is presented.

Table 1. Flow cytometric analysis of cell-surface markers on pulp and adipose derived $CD105^+$ cells and total pulp cells at the third passage of culture.

	Pulp $CD105^+$ Cells	Adipose $CD105^+$ Cells	Total Pulp Cells
CD24	1.8%	1.7%	0.3%
CD29	95.9%	90.5%	99.2%
CD31	0%	0%	0%
CD33	3.7%	0%	0.2%
CD34	45.5%	0.1%	47.1%
CD44	96.2%	92.3%	99.9%
CD73	97.2%	0.8%	22.3%
CD90	98.1%	95.6%	97.5%
CD105	98.5%	74.0%	4.6%
CD146	0.8%	0.2%	0.9%
CD150	2.3%	0.2%	0.9%
MHC class I	36.0%	80.0%	73.8%
MHC class II	0.4%	0%	0.4%
CXCR4	12.2%	5.9%	5.3%

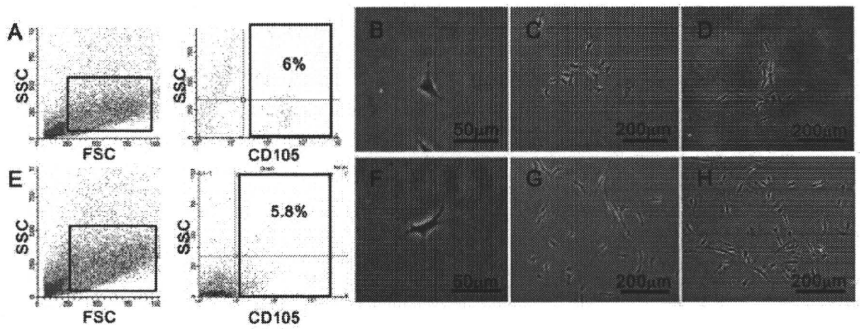

Nakashima. Fig 1

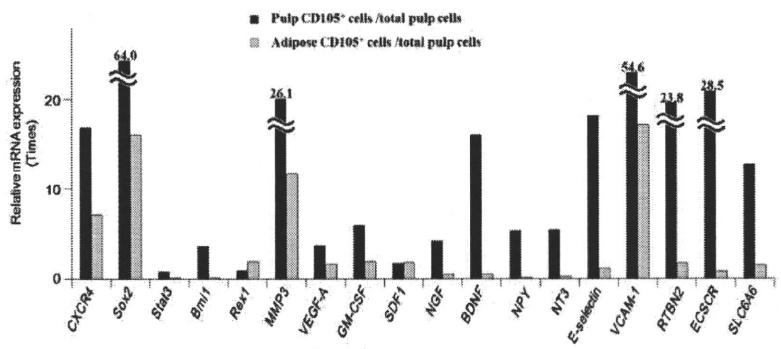

Nakashima. Fig 2

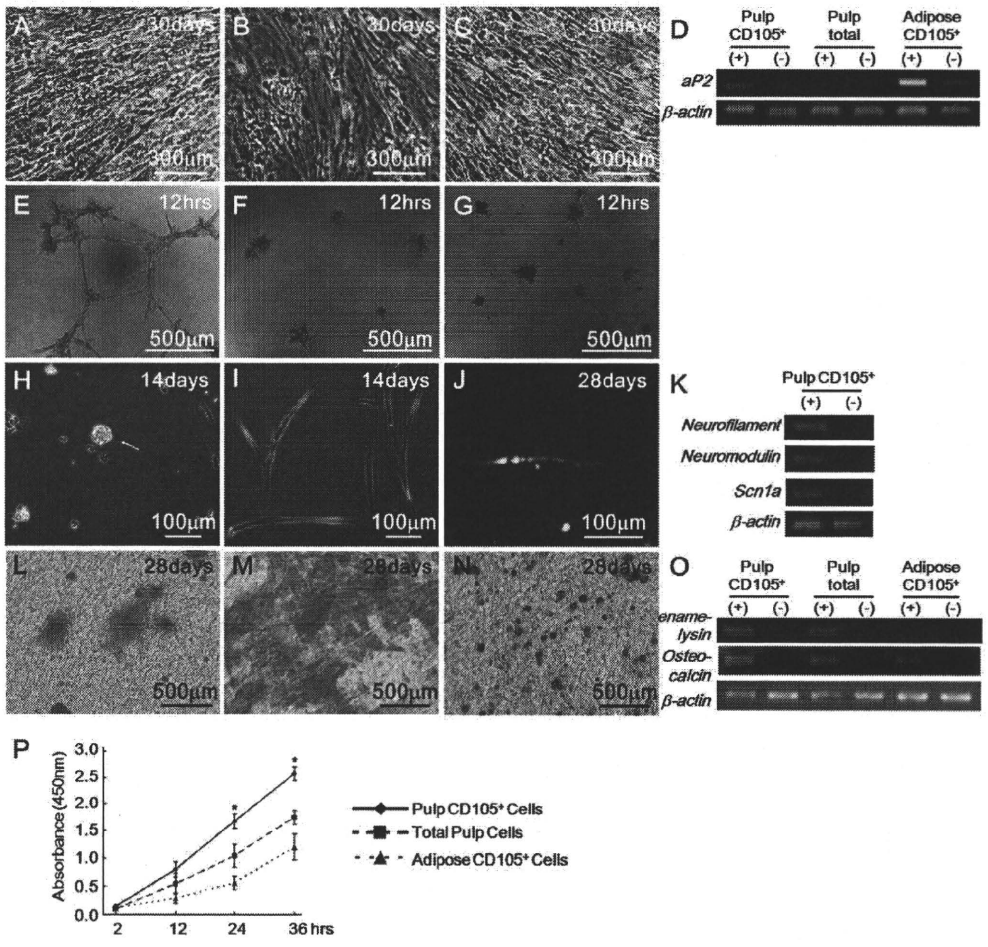

Nakashima. Fig 3

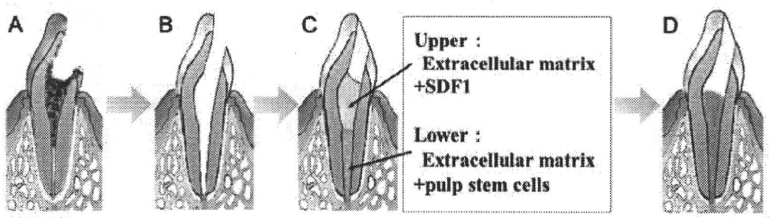

Nakashima. Fig 4

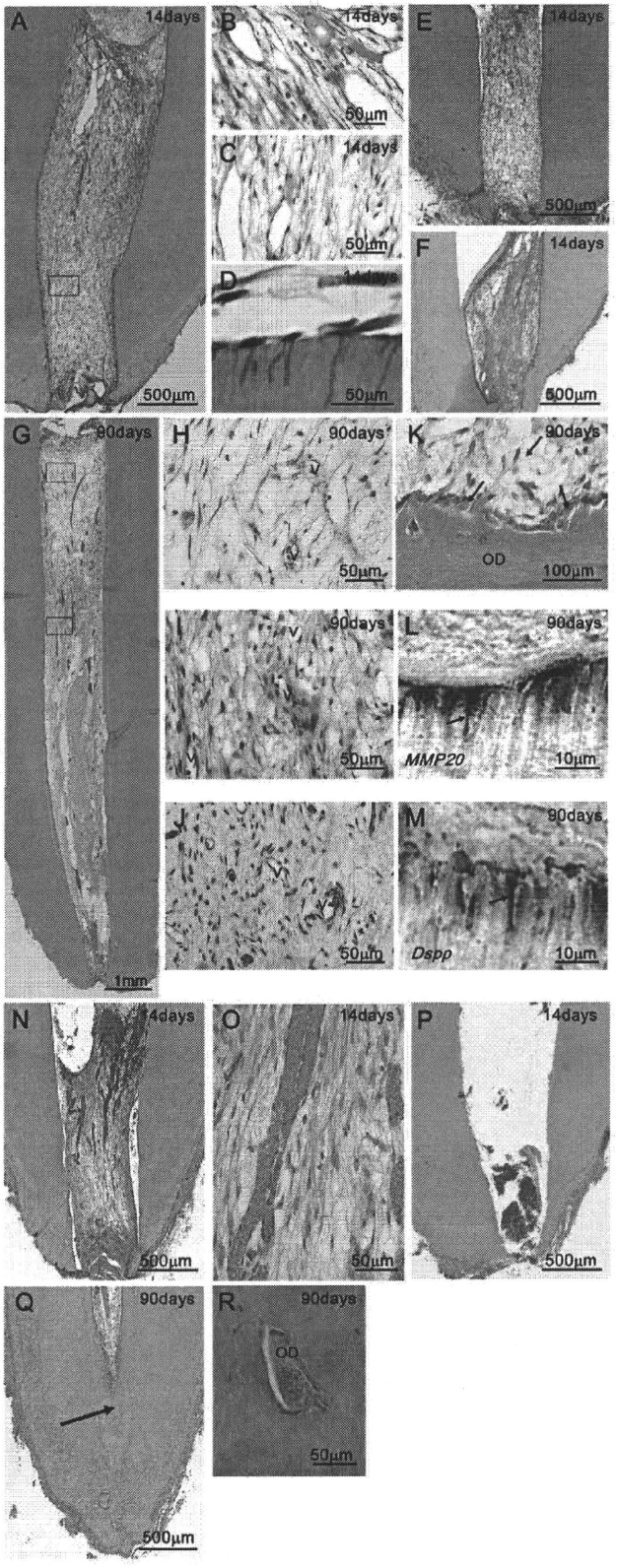

Nakashima. Fig 5

Tissue Engineering Part A
Complete pulp regeneration after pulpectomy by transplantation of CD105⁺ stem cells with SDF-1 (doi: 10.1089/ten.TEA.2010.0615)

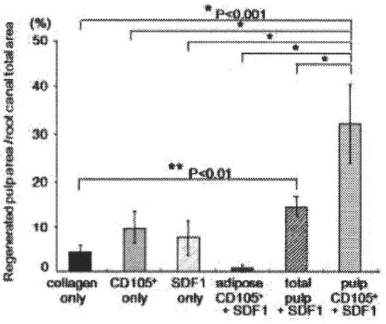

Nakashima. Fig 6

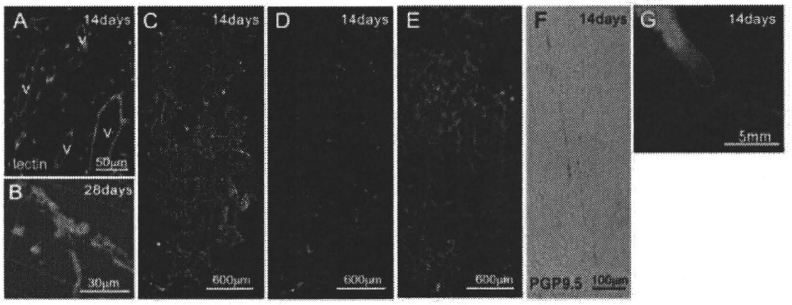

Nakashima. Fig 7

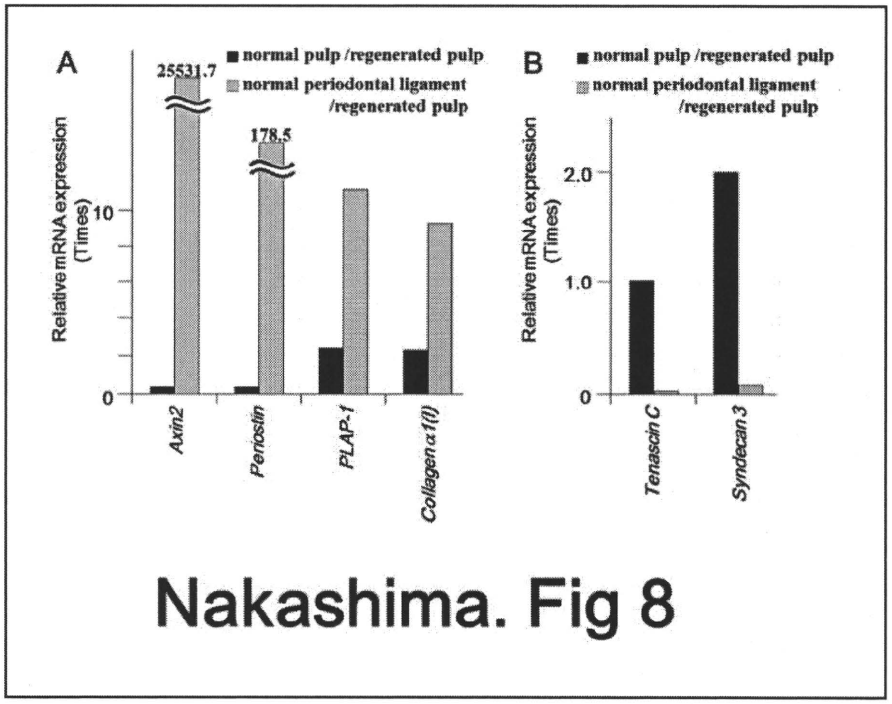

Vol 465|13 May 2010|doi:10.1038/nature09017

ARTICLES

Aberrant silencing of imprinted genes on chromosome 12qF1 in mouse induced pluripotent stem cells

Matthias Stadtfeld[1,2,3]*, Effie Apostolou[1,2,3]*, Hidenori Akutsu[4], Atsushi Fukuda[5], Patricia Follett[1], Sridaran Natesan[6], Tomohiro Kono[5], Toshi Shioda[2] & Konrad Hochedlinger[1,2,3]

Induced pluripotent stem cells (iPSCs) have been generated by enforced expression of defined sets of transcription factors in somatic cells. It remains controversial whether iPSCs are molecularly and functionally equivalent to blastocyst-derived embryonic stem (ES) cells. By comparing genetically identical mouse ES cells and iPSCs, we show here that their overall messenger RNA and microRNA expression patterns are indistinguishable with the exception of a few transcripts encoded within the imprinted *Dlk1–Dio3* gene cluster on chromosome 12qF1, which were aberrantly silenced in most of the iPSC clones. Consistent with a developmental role of the *Dlk1–Dio3* gene cluster, these iPSC clones contributed poorly to chimaeras and failed to support the development of entirely iPSC-derived animals ('all-iPSC mice'). In contrast, iPSC clones with normal expression of the *Dlk1–Dio3* cluster contributed to high-grade chimaeras and generated viable all-iPSC mice. Notably, treatment of an iPSC clone that had silenced *Dlk1–Dio3* with a histone deacetylase inhibitor reactivated the locus and rescued its ability to support full-term development of all-iPSC mice. Thus, the expression state of a single imprinted gene cluster seems to distinguish most murine iPSCs from ES cells and allows for the prospective identification of iPSC clones that have the full development potential of ES cells.

Induced pluripotent stem cells (iPSCs), generated by the overexpression of transcription factors such as Oct4 (also called Pou5f1), Sox2, Klf4 and c-Myc in somatic cells[1,2], have enormous therapeutic potential as they enable the derivation of patient-specific pluripotent cell lines to study and possibly treat degenerative diseases. Although the generation of iPSCs is technically simple and ethically uncontroversial, it remains unclear whether iPSCs are molecularly and functionally different from ES cells derived from blastocysts, which are considered the gold standard for pluripotent cells. Previously published reports indicate high similarities between ES cells and iPSCs, including indistinguishable global histone modification and DNA methylation patterns[3,4]. In addition, iPSCs, like ES cells, give rise to numerous differentiated cell types, including the germ line, in the context of chimaeric animals[5,6]. More recently, iPSCs have been shown to support the development of all-iPSC mice using tetraploid (4n) embryo complementation[7–9], the most stringent assay for developmental potential[10,11].

Despite these similarities, there is emerging evidence for substantial differences between ES cells and iPSCs. For example, most iPSC clones give rise to low-grade chimaeras after injection into diploid blastocysts and fail to support the development of postnatal all-iPSC mice upon 4n embryo complementation[12–14]. At the molecular level, major differences in mRNA and microRNA (miRNA) expression[15–17], as well as in DNA methylation[18–20], have been reported between ES cells and iPSCs. These observations indicate that factor-mediated reprogramming results in abnormalities in resultant iPSCs, which could impede their therapeutic utility. In contrast, nuclear-transfer-mediated reprogramming gives rise to nuclear transfer ES cells that are molecularly and functionality indistinguishable from ES cells derived from fertilized embryos[21,22], raising the possibility that nuclear transfer generates cells that are more completely reprogrammed than iPSCs.

A potential limitation of the aforementioned studies is that ES cells were compared with iPSCs of different genetic backgrounds and harbouring viral transgenes, which are known to affect gene expression patterns[21,23] and the functionality[1,6] of cells. We therefore revisited the question of whether ES cells and iPSCs are equivalent by comparing genetically matched cell lines.

Transcriptional comparison of ES cells and iPSCs

To circumvent the potentially confounding effects of genetic background and viral integrations on gene expression patterns and developmental potential, we used a novel transgenic reprogramming system to generate genetically matched mouse ES cells and iPSCs[24]. Briefly, a polycistronic cassette expressing Oct4, Klf4, Sox2 and c-Myc[25] (OKSM) under the control of a doxycycline-inducible promoter was inserted into the collagen type I α1 (*Col1a1*) locus of ES cells expressing the reverse tetracycline-dependent transactivator (rtTA) from the *ROSA26* promoter[26]. These collagen-OKSM ES cells were then used to generate mice from which different somatic cell types were isolated and induced with doxycycline to derive genetically matched iPSCs for molecular and functional comparisons (Fig. 1a, b).

[1]Howard Hughes Medical Institute at Massachusetts General Hospital, Center for Regenerative Medicine; Harvard Stem Cell Institute, 185 Cambridge Street, Boston, Massachusetts 02114, USA. [2]Massachusetts General Hospital Cancer Center and Harvard Medical School, 149 13th Street, Charlestown, Massachusetts 02129, USA. [3]Department of Stem Cell and Regenerative Biology, Harvard University and Harvard Medical School, 42 Church Street, Cambridge, Massachusetts 02138, USA. [4]Department of Reproductive Biology, National Institute for Child Health and Development, Tokyo 157-8535, Japan. [5]Department of BioScience, Tokyo University of Agriculture, Tokyo 156-8502, Japan. [6]Sanofi-Aventis, 270 Albany Street, Cambridge, Massachusetts 02139, USA.
*These authors contributed equally to this work.